Cancer Chemother Pharmacol (2011) 68:359–369
DOI 10.1007/s00280-010-1492-9

ORIGINAL ARTICLE

Conjugation of chlorin p_6 to histamine enhances its cellular uptake and phototoxicity in oral cancer cells

Arpana Parihar · Alok Dube · P. K. Gupta

Received: 23 June 2010 / Accepted: 8 October 2010 / Published online: 27 October 2010

Abstract
Purpose Our previous studies in hamster cheek pouch model have shown that chlorin p_6 (Cp_6), a chlorophyll derivative is a suitable photosensitizer for photodynamic treatment (PDT) of small tumors (<5 mm). However, for bigger tumors, the accumulation of Cp_6 was inadequate, which compromised the effectiveness of PDT. The purpose of present study was to investigate the possibility of improving the cellular uptake of Cp_6 by conjugating it to histamine, a biogenic amine that is known to modulate tumor growth and development via cell surface receptors.
Methods The conjugate of Cp_6 and histamine (Cp_6-his) was prepared by carbodiimide coupling reaction. Cellular uptake, intracellular localization and cytotoxicity of both Cp_6 and its conjugate were investigated in two human oral cancer cell lines (4451 and NT8e). The percentage of necrotic and apoptotic cells after PDT were also estimated using Hoechst 33342–propidium iodide staining.
Results In both the cell line, the cellular uptake of Cp_6-his was found to be ~10 times higher when compared to Cp_6. Histamine led to a slight increase in intracellular uptake of Cp_6-his, whereas ranitidine, a histamine H2 receptor antagonist, and incubation at lower temperature (~15°C) led to its inhibition, suggesting that uptake of Cp_6-his is receptor mediated. Results on western blot confirmed the presence of H2 receptor in both the cell line. Observations on intracellular localization revealed that unlike Cp_6, which localized on multiple sites, Cp_6-his showed localization on the cell membrane and around the perinuclear region. Moreover, the phototoxicity induced by Cp_6-his was ~4 times higher when compared to Cp_6 in both the cell lines. There was, however, no significant difference in the mode of cell death.
Conclusion Results suggest that conjugating Cp_6 with histamine can help improve the effectiveness of PDT in oral cancer cells by enhancing its intracellular delivery.

Keywords Chlorophyll derivative · Photodynamic therapy · Mode of cell death · Targeted delivery

Introduction

Photodynamic therapy (PDT) is a clinically approved modality for the treatment of cancer and non-oncological disorders [1]. The anticancer effect of PDT is based on the generation of cytotoxic reactive oxygen species by the interaction of light with the photosensitive drug. PDT offers dual selectivity: first, due to the preferential accumulation of the photosensitizer in tumor and second, by limiting the light exposure to the diseased region [2]. In past decade, photosensitizers derived from plant pigment 'chlorophyll-*a*' have received considerable attention for PDT because these show good absorption coefficient in the wavelength region of therapeutic interest (660–800 nm) and provide efficient singlet oxygen generating capability necessary for achieving the effective PDT outcome [3].

We have previously shown that chlorin p_6 (Cp_6), a chlorophyll derivative, is a promising photosensitizer for photodynamic treatment (PDT) of chemically induced tumors in hamster cheek pouch model [4]. However, for systemic administration of the drug (1.5 mg/kg), while the uptake of Cp_6 was good for small tumors (<5 mm), for bigger tumors its accumulation was inadequate, which compromised the

A. Parihar · A. Dube (✉) · P. K. Gupta
Laser Biomedical Applications and Instrumentation Division,
Raja Ramanna Center for Advanced Technology,
Laser R & D Block 'D', Indore, MP 452013, India
e-mail: okdube@rrcat.gov.in

PDT efficacy. A promising approach to improve the tumor selectivity and PDT efficacy of photosensitizer is to conjugate it with molecules that can interact with tumor cells specifically via cell surface receptors [5, 6]. This approach utilizes the fact that tumor cells typically have increased expression of cell surface receptors for various growth factors or regulatory biomolecules. For example, photosensitizer conjugated to low-density lipoprotein (LDL), transferrin, insulin and epidermal growth factor (EGF) have been investigated in various studies [5, 6].

In the present study, we have examined the possibility to exploit histamine receptors for improving delivery and photodynamic efficacy of Cp_6 in oral cancer cell lines. Histamine is a biogenic amine, which apart from its classical role in gastric acid secretion, inflammation, immunomodulation and in nervous regulation [7], has also been suggested to play an important role in tumor growth and development [8–10]. It has been reported that cancer cells produce high levels of histamine and the ability to regulate cell proliferation via expression of histamine receptors [10]. Studies in melanoma have shown a positive correlation between histamine production and histamine receptor expression, suggesting up-regulation of histamine receptors and existence of autocrine control of melanoma progression by histamine [11]. Elevated levels of histamine receptors in malignant tissue almost 2–5 times higher than normal tissue have been reported in several types of malignancies e.g., breast carcinoma [12], melanoma [12] and adrenocortical cancer [13]. The expression of histamine receptor H1 and H2 has been found in several human cancer cell lines of different tumor types such as mammary carcinomas, melanoma, gliomas, colon carcinoma, leukemia, pancreatic carcinoma, ovarian carcinoma, gastric carcinoma, epidermoid and uterine carcinoma. [10]. To utilize histamine receptors for delivery of Cp_6 in cancer cells, we coupled the 17′-carboxylic group of Cp_6 with amino group of the histamine via a peptide linkage utilizing standard carbodiimide coupling reaction. The cellular uptake, intracellular localization and phototoxicity of both Cp_6 and Cp_6-histamine conjugate have been compared. In order to find out the presence of histamine receptor, western blot was performed. Also, the effects of low temperature, agonist and antagonist on cellular uptake of cp6-his or cp6 were measured. The percentage of necrotic and apoptotic cells after PDT was estimated using Hoechst 33342–propidium iodide staining.

Materials and methods

Preparation of Cp_6 and Cp_6-histamine conjugate

Chlorophyll-*a* was extracted from dry spinach leaves and converted into Purpurin-18 (Pp-18) following the procedure described by Hoober et al. [14]. The Pp-18 was conjugated to histamine by standard carbodiimide coupling reaction. In brief, Pp-18 (2 mg, 1.5 mM) was dissolved in dry DCM (2.5 mL) and mixed with 3 mM 1-ethyl-3-(3-dimethylaminopropyl)-carbodiimide (EDC) under continuous stirring. After 10 min, a solution of histamine hydrochloride (0.9 mM) in methanol (5 ml) was added drop wise and the solution was stirred at room temperature for 24 h. The crude reaction mixture was loaded directly onto a silica gel column and eluted using a mixture of DCM/MeOH 95:5 with 1% of triethylamine (TEA). The dark red solution eluted from the column was washed with water to remove the triethylammonium salt impurity. The organic phase containing Pp18–histamine conjugate was evaporated to dryness and converted into Cp_6-his by hydrolytic cleavage of the anhydride ring of Pp-18 using alkaline methanol. The resultant green solution was loaded onto silica gel column and eluted with MeOH/DCM (90:10). The faster eluting fraction containing Cp_6-his was collected and dried under vacuum. The purity of the conjugate was checked by thin layer chromatography (TLC) on preparative silica gel plate using 90% aqueous methanol as mobile phase. Mass spectrum of Cp_6-his was obtained at IIT, Mumbai India.

Absorption and fluorescence spectra

Cp_6 and Cp_6-his were dissolved in ethanol: PEG(400): HEPES buffer (20:30:50) to obtain the absorption and fluorescence emission spectra. The absorption spectra were recorded from 250 to 750 nm using 1-nm band-pass on a Cintra-20 spectrophotometer (GBC, Australia). Fluorescence measurements were done using a Fluorolog-2 spectrofluorometer (Spex, USA). The samples were illuminated with 400 nm light, and fluorescence emission was scanned from 600 to 750 nm keeping both excitation and emission slits at 1 mm corresponding to a band-pass of 3.6 and 1.8 nm, respectively.

Cancer cell culture

Human oral squamous cell carcinoma (OSCC) cell line NT8e derived from tumor specimen of the upper aerodigestive tract (pyriform fossa) was obtained from Cancer research Institute, Tata Memorial Hospital, Mumbai, India. Cell line 4451, a squamous carcinoma cell line derived from a recurrent tumor in the lower jaw, was obtained from Institute of Nuclear Medicine and Allied Sciences, Delhi, India. The cells were maintained in DMEM containing essential amino acids, 25 mM *N*-2-hydroxyethylpiperazine-*N*′-2-ethanesulphonic acid (HEPES), 10% fetal bovine serum and antibiotics. The cells were grown in monolayer at 37°C in humidified incubator (Nuaire, USA) under 5% CO_2–95% air atmosphere. The cells were harvested by

trypsinization, re-suspended in culture media and plated either in plastic Petri dishes or in 96-microwell plate. After ~18 h of growth, the cells in log phase were used for all further experiments.

Photosensitizer treatment

Cp_6-his is hydrophilic and can be dissolved in aqueous solutions, but storage at physiological pH (7.4) results in its partial aggregation. Solubilization in alkaline buffer (pH 9.0) containing PEG-400 maintains it in the monomeric state because the molecule remains in anionic form at this pH. Therefore, Cp_6-his was first dissolved in ethanol and then reconstituted in HEPES buffer (10 mM, pH 9.0) containing 30% PEG-400. For comparison, stock solution of Cp_6 was also made in the same system.

The cells grown in microplate wells or culture Petri dishes were treated with Cp_6-his or Cp_6 by adding their specified concentrations in growth medium (DMEM with 10% serum) followed by incubation at 37°C in a 5% CO_2, 95% air atmosphere for different time periods varying from 1/2 to 7 h. The cellular uptake of Cp_6 or Cp_6-his was also measured in the presence of histamine (1 and 5 mM), ranitidine (100 μM) and pheniramine (100 μM), and the incubation time used in this case was 3 h. For studies on cellular uptake of photosensitizer at lower temperature, the microplates were placed on a refrigerant gel pack pre-cooled to ~12°C in a thermocol box and the box was transferred to 5% CO_2, 95% air atmosphere inside the CO_2 incubator. The temperature and the pH of the culture media measured before and after 3-h incubation remained nearly constant.

Extraction and estimation of photosensitizer content in cells

At the end of each incubation time point, the culture supernatant was aspirated and the cell monolayer was washed twice with cold PBS. To extract the photosensitizer from the cells, 250 μl detergent solution (0.1 M NaOH containing 0.1% SDS) was added in each well and the cell monolayer was scrapped with plastic pipette tip. The detergent solution was pipetted several times to make a homogenous cell suspension. After 60 min incubation at room temperature to allow complete solubilization, the solution was mixed with 750 μl PBS and centrifuged at 6,900 *g* for 10 min. The supernatant from each sample was collected and used for fluorescence measurements. Fluorescence spectra were recorded from 610 to 750 nm keeping excitation wavelength at 400 nm. The relative fluorescence intensity at 674 nm was measured and used to estimate the concentration of the photosensitizer from a standard curve. The concentration of the photosensitizer was normalized with respect to the total protein content estimated by the Lowery's method. The cell number was kept approximately equal in each experiment for comparison purpose.

Photodynamic treatment

The cells were incubated with Cp_6-his or free Cp_6 as described above. After incubation for 3 h, the cell monolayer was washed twice with DMEM medium (no serum), followed by addition of fresh growth medium. The cells were irradiated with red light (660 ± 25 nm) using light source LC-122A (Ci tek, USA) coupled to optical fiber probe (Dia. 1.2 cm, length 1 m) with an in-built narrow band-pass filter. The distal end of fiber optic probe was placed at a height of ~14 cm to expand the beam area for illumination of the entire microplate or three culture dishes simultaneously. The light intensity measured by a power meter model AN/2 (Ophir) at the sample position was ~79 W/m^2. The light dose was varied by changing the irradiation time from 0–8 min corresponding to irradiation dose of 0–38 kJ/m^2.

Measurements on phototoxicity

For determination of phototoxicity, cell viability was measured by MTT assay [15]. Nearly 18 h after irradiation, the growth medium was removed and 100 μl DMEM medium (w/o serum) containing MTT (5.0 mg/ml) was added to each well. After 4-h incubation, the medium was removed and the formazan crystals formed within cells were solubilized by addition of 0.4 N hydrochloric acid in isopropanol. The optical density of the blue solution was measured at 570 and 690 nm using a microplate reader (Power Wave 340, Bio-tek Instruments Inc., USA). Phototoxicity was calculated as the percent decrease in MTT reduction with respect to a control sample, which received no photosensitizer and no light.

Intracellular localization of photosensitizer

The cells were grown on gelatin-coated glass coverslips and incubated with the photosensitizers for 3 h. After washing with DMEM medium, the coverslips were mounted onto the stage of an inverted microscope (Olympus, Japan) and the cells were observed at 100× magnification using an epifluorescence illumination set up (excitation 530–560 nm, long-pass filter 580 nm). The images were recorded using a CCD Camera Model 'ProgRes CFscan' and a ProgRes Capture Pro software (Jenoptik, Germany).

Western Blot for detection of histamine H2 receptor

The cells were solubilized by incubation in a sample buffer (50 mM Tris–HCl, 2% SDS, 100 mM 2-mercaptoethanol,

10% glycerol and 0.05% bromophenol blue, pH 6.8) at 100°C for 5 min. The aliquots of cell extract were electrophoresed in 12% SDS–PAGE gel and transferred to nitrocellulose membranes using a semidry electroblotting apparatus (Hoefer). The residual binding sites were blocked with 5% non-fat powdered milk in PBST (phosphate-buffered saline containing 0.05% Tween 20), and membranes were incubated with (Dilution, 1:400) polyclonal rabbit anti-H2 receptor antibody (Santa Cruz Biotechnology, Santa Cruz, CA) in PBST. All subsequent washes were performed with the same buffer. Reactivity was developed using an (Dilution, 1:5,000) goat anti-rabbit IgG linked to horseradish peroxidase (Millipore) via enhanced chemiluminescence reagents (Amersham Biosciences).

Assessment of apoptosis and necrosis

Percentage of cells undergoing apoptosis and necrosis following photodynamic treatment was determined by fluorescence microscopy. In brief, ~18 h after PDT, the cells were incubated with Hoechst (final concentration 10 μg/ml) and propidium iodide (final concentration 20 μg/ml) in the medium. After 5 min, the cells were observed under epifluorescent microscope (Olympus, Japan) using a fluorescent filter cube (excitation 340–380 nm, barrier filter 430 nm). Cell stained with Hoechst showing characteristic chromatin condensation and fragmentation were identified as apoptotic cells. Cells showing red fluorescence of PI indicated loss of plasma membrane integrity and therefore identified as necrotic cells. A minimum of 500 cells were counted in both control as well as each treatment group. Percentage of apoptotic and necrotic cells was calculated from the total number of cells counted.

Statistical analysis

The data are expressed as average ± SD of the values obtained from three independent experiments. For data on the cellular uptake of Cp_6 or Cp_6-his either in room temperature and in low temperature or in the absence or presence of histamine, ranitidine and pheniramine, Student's *t*-test was applied to test the significance of the difference between control and the treatment. A level of $P < 0.01$ and $P < 0.05$ was considered to be statistically significant.

Results

Characterization of the conjugate

The purity of Cp_6-his was checked by thin layer chromatography (TLC) on preparative silica gel plate using 95% methanol as mobile phase. The results of TLC show that Cp_6-his separated as a single spot on silica gel plates with retardation factor (Rf) of ~0.9 and in comparison, the Rf for Cp_6 was ~0.1 (Fig. 1a). The mass spectrum of the conjugate gave anticipated molecular ion peak at 719.8 (calculated mass 719.76 for disodium salt C38H39N7Na2O5) (Fig. 1b). The chemical structures of Cp_6 and its conjugate are shown in Fig. 1c.

Figure 2 shows the absorption spectra of free Cp_6 and Cp_6-his dissolved in ethanol:PEG(400):buffer system. Attachment of histamine to Cp_6 did not cause any major change in its absorption peak positions in visible region except that the q band position was slightly red shifted to 666 from 663 nm. The molar absorption coefficient of Cp_6-his was estimated to be 42,314 and 12,750 M^{-1} cm^{-1} at soret and *q* band position, which is ~1/2 of the molar absorption coefficient of Cp_6 at the same wavelengths. The 400 nm excited fluorescence of Cp_6 and Cp_6-his is shown in inset.

Intracellular uptake of Cp_6 and Cp_6-his

The kinetics of intracellular uptake of Cp_6 (5 μM) and Cp_6-his (5 μM) in 4451 and Nt8e cells is shown in Fig. 3. In both the cell lines, the uptake of Cp_6 was seen to increase up to 1 h and saturated thereafter. In case of Cp_6-his, cellular uptake showed an initial rise till 1 h followed by a slower phase of increase up to 5 h. The intracellular concentration of Cp_6-his was noticeably higher when compared to Cp_6 by a factor of 5 and 10 at 1- and 3-h incubation, respectively.

The effects of histamine (1 and 5 mM), ranitidine (100 μM) and pheniramine (100 μM) on the cellular uptake of Cp_6-his and Cp_6 are shown in Fig. 4. Cells were incubated with each photosensitizer (5 μM) alone and in combination with above test compounds for 3 h. In the presence of histamine, a significant increase ($P < 0.01$) in cellular uptake of Cp_6-his was observed in both the cell lines (Fig. 4a). Addition of histamine H2 receptor antagonist ranitidine led to ~30% reduction (P value < 0.01) in the cellular uptake of Cp_6-his, whereas pheniramine, a histamine H1 receptor antagonist showed less inhibition (15–20%, P value < 0.05) (Fig. 4b). For Cp_6, no significant change in the cellular uptake was observed in the presence of any of these compounds (Fig. 4a, b).

Figure 5 shows the effect of lower temperature on the cellular uptake of Cp_6-his and Cp_6 in the presence or absence of 10% serum in the culture medium. The cellular uptake of both Cp_6-his and Cp_6 was found to decrease due to incubation of cells at lower temperature and in the presence of serum in the medium (Fig. 5a). The percent inhibition was slightly higher for Cp_6-his (50–60%) when compared to Cp_6 (30–40%). When serum is omitted from the culture medium, the inhibition in cellular uptake due to

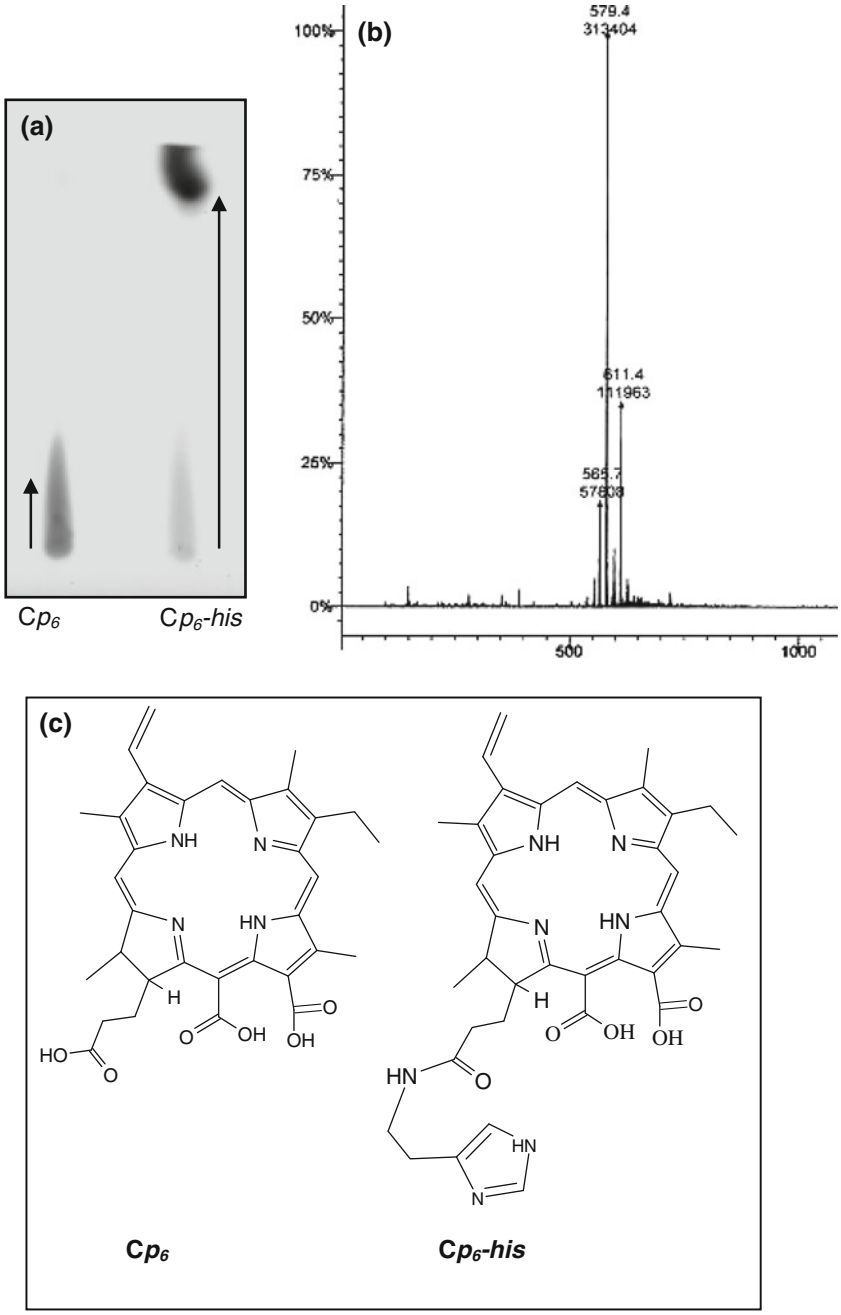

Fig. 1 Photograph of TLC plate showing mobility of Cp_6 and Cp_6-his after chromatography using 90% methanol as mobile phase (**a**). Mass spectrum of Cp_6-his showing heaviest molecular ion peak at 719.8 (**b**). Chemical structure of Cp_6 and Cp_6-his (**c**)

lower temperature was found to almost diminish in case of Cp_6 (7–10%), whereas for Cp_6-his, it remained nearly same (40%) (Fig. 5b).

Detection of histamine receptor in cells

In order to find out the presence of histamine receptor in oral cancer cell lines, western blot was performed. Immunoblotting with H2 receptor antibody revealed four bands with molecular masses of approximately 30, 60, 80 and 100 kDa (Fig. 6). The presence of four bands for H2 receptor is in agreement with the previous studies and suggests presence of oligomeric form of H2 receptors with actual molecular masses of 31.5 kDa [16].

Intracellular localization

In Fig. 7, the bright field (left panel) and fluorescence images (right panel) of 4451 and Nt8e cells showing cell morphology and intracellular localization of Cp_6 and Cp_6-his are displayed. In both the cell lines, the fluorescence of Cp_6 was observed in punctuated granular structures, indicating its localization at multiple sites inside the cells Fig. 7b, f. The intracellular localization of Cp_6-his was

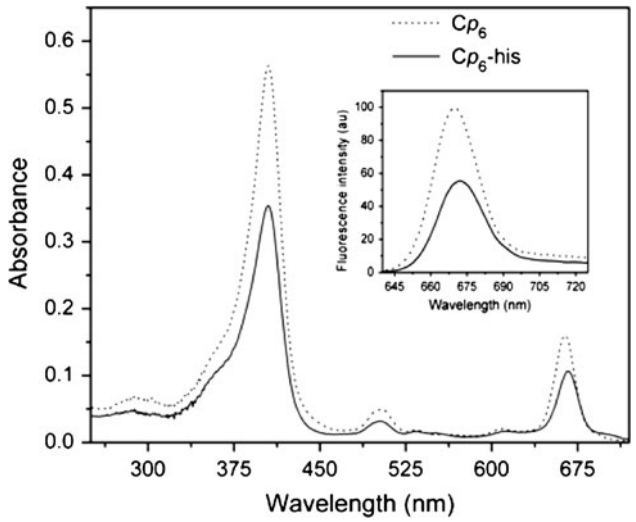

Fig. 2 Absorption spectra of Cp_6 and Cp_6-his in Ethanol:PEG:Water system. Respective fluorescence emission spectra are shown as *Inset*

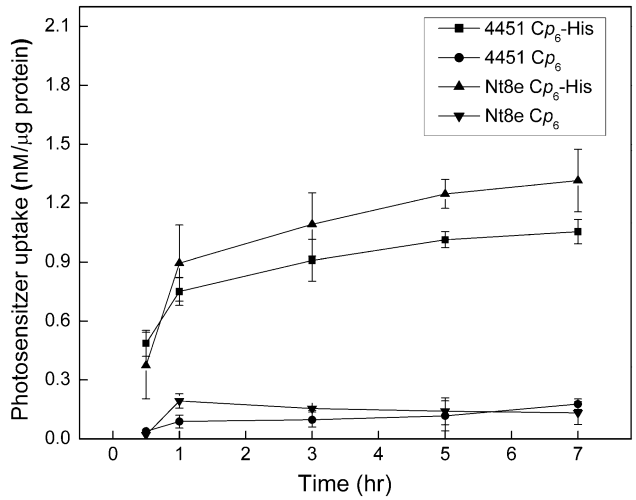

Fig. 3 Time-dependent cellular uptake of Cp_6 and Cp_6-his Conjugate in 4451 and Nt8e cells. Cells were incubated with 5 μM of Cp_6 and Cp_6-his each for different time periods (0.5–7 h). Each data point represents the average ± SD of values obtained from three independent experiments

noticeably different from Cp_6 (Fig. 7d, h). The fluorescence of Cp_6-his in 4451 cells is observed in discrete vesicle type structures around the perinuclear region of the cytoplasm (Fig. 7d). While Nt8e cells displayed the fluorescence of Cp_6-his within granular structures as diffused patch near the nucleus (Fig. 7h). In both the cell lines, the fluorescence labeling of the cell membrane by Cp_6-his is also clearly visible (Fig. 7d, h). Moreover, the fluorescence of Cp_6-conjugate was much more intense when compared to the fluorescence of Cp_6 due to higher uptake. The brightness and contrast of the images shown in Fig. 7 were adjusted for proper visualization of the intracellular localization of Cp_6 and Cp_6-his.

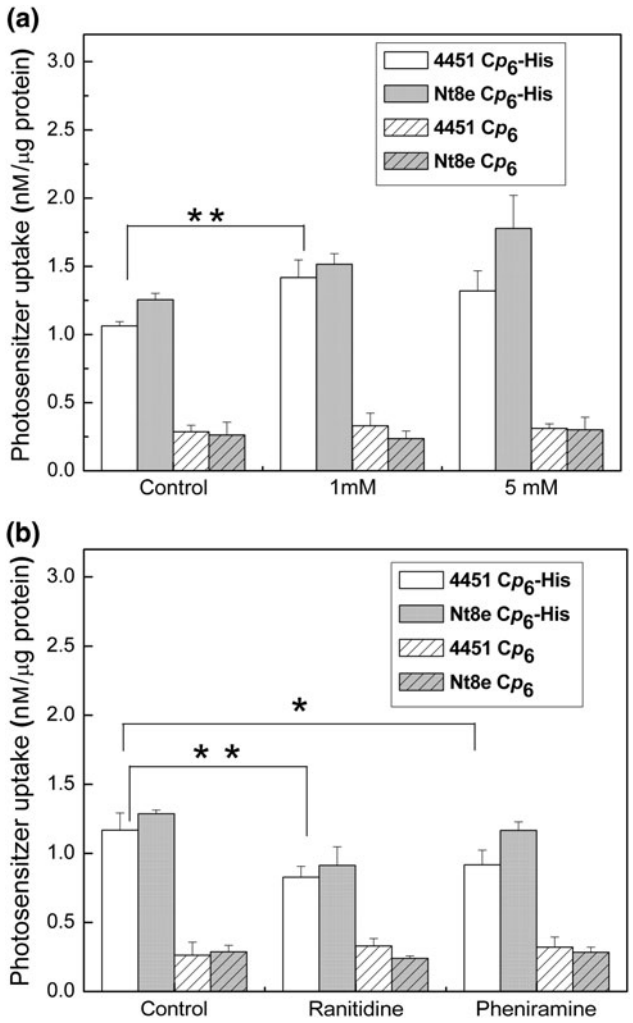

Fig. 4 The effect of histamine (**a**) and histamine receptor antagonist (**b**) on the cellular uptake of Cp_6 and Cp_6-his conjugate. Cells were incubated with 5 μM Cp_6 and Cp_6-his alone or with histamine (1 and 5 mM), ranitidine (100 μM) and pheniramine (100 μM) for 3 h. Each data point represents the average ± SD values obtained from three independent experiments. (*P value < 0.05, **P value < 0.01)

Phototoxicity

The phototoxicity of Cp_6-his was determined by subjecting the cells to photodynamic treatment using different concentrations of the conjugate and a fixed red light irradiation dose at 28 kJ/m^2. Percent phototoxicity was measured with respect to a control sample that received no drug and no light exposure, and these results are presented in Fig. 8. The percent phototoxicity can be seen to increases in a concentration-dependent manner in both 4451 and Nt8e cell lines. The concentration of Cp_6-his required to obtain 95% phototoxicity at the light dose of 28 kJ/m^2 was found to be 5 μM (Fig. 8a). To compare the effectiveness of Cp_6-his with Cp_6, both the cell lines were subjected to photodynamic treatment using same concentration (5 μM) and variable light dose (0–38 kJ/m^2). The results presented in Fig. 8b

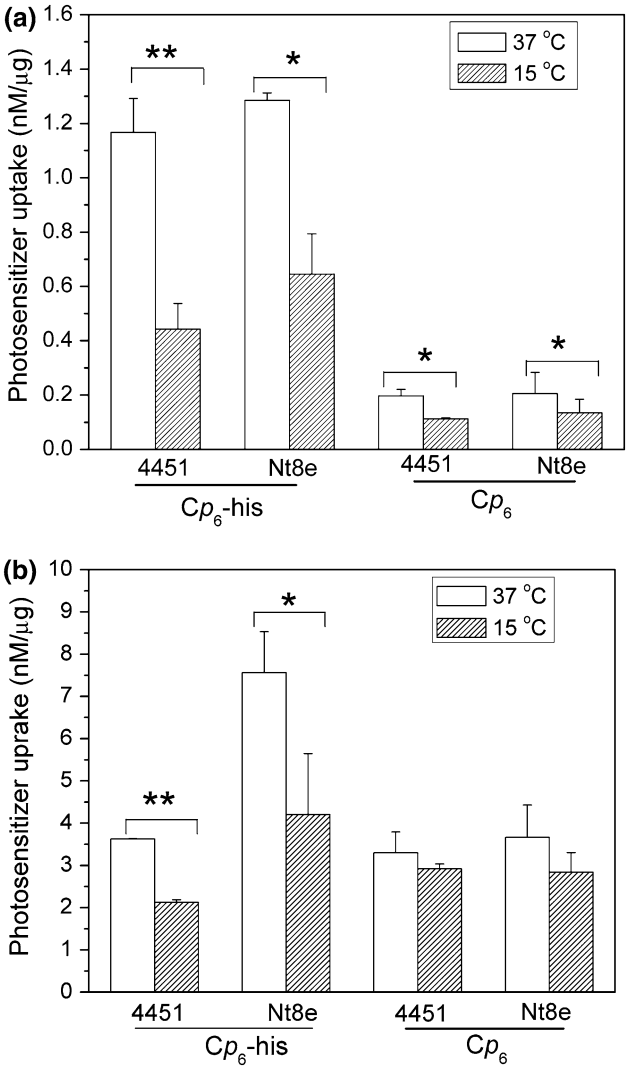

Fig. 5 The effect of temperature on the cellular uptake of Cp_6 and Cp_6-his conjugate. Cells were incubated with 5 μM Cp_6 and Cp_6-his at 37°C or 15°C in culture medium containing 10% serum (**a**) or without serum (**b**). Each data point represents the average ± SD values obtained from three independent experiments. (*P value < 0.05, **P value < 0.01)

show that for a given light dose, the phototoxicity was much higher with Cp_6-his than Cp_6. The light dose required to achieve 50–60% cell killing was ~12 and 32 kJ/m^2 for Cp_6-his and Cp_6, respectively. At 28 kJ/m^2 light dose, the phototoxicity induced by Cp_6-his was ~95% and in comparison, Cp_6 led to ~50% phototoxicity. These data clearly show that Cp_6 conjugate is more effective than Cp_6. No dark toxicity was noticed for either Cp_6-his or Cp_6 at the concentration used.

Mode of cell death induced by Cp_6-his

A comparison of the relative magnitude of necrosis or apoptotic cell death in both the cell lines treated with Cp_6 or

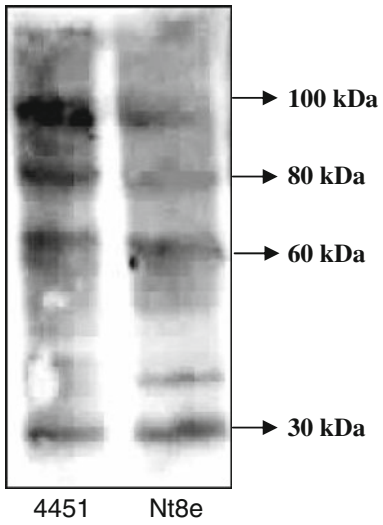

Fig. 6 Image of nitrocellulose membrane showing presence of H2 receptor in 4451 and Nt8e cells after western blot of the cellular protein using polyclonal rabbit anti-H2 receptor antibody and HRP-conjugated goat anti-rabbit IgG and detection via enhanced chemiluminescence reagents

Cp_6-his is shown in Fig. 9. There was no major difference between the PDT treatment by Cp_6 and Cp_6-his with respect to the percentage of apoptotic or necrotic cells in both the cell lines. Also, in both the cases, the cell line 4451 showed higher percentage of necrotic cells when compared to Nt8e cells, for which the percentage of apoptotic cells in turn was more.

Discussion

The motivation for the present study was to investigate the use of histamine, a biogenic amine to enhance the uptake and tumor selectivity of Cp_6 by exploiting histamine receptors for delivery of photosensitizer in cancer cells. The results of cellular uptake studies presented in Fig. 3 show that the Cp_6-his is taken up more efficiently by the cells than free Cp_6. To check whether the uptake occurred via histamine receptors, we also measured the cellular uptake of Cp_6-his in the presence of histamine. Instead of the expected inhibition, histamine led to slight increase in the uptake of Cp_6-his (Fig. 4a). The reason for this effect is presently not clear. Based on the fact that the receptor affinity of some agonist/antagonist is higher than histamine [17], one can assume Cp_6-his to have stronger receptor affinity, which prevented histamine to compete efficiently for the binding site. Moreover, there is also a possibility that histamine can up-regulate expression of its receptors [11]. The observed increase in the uptake of Cp_6-his by histamine could involve these effects. Therefore, to find out the involvement of histamine receptors, cellular uptake of

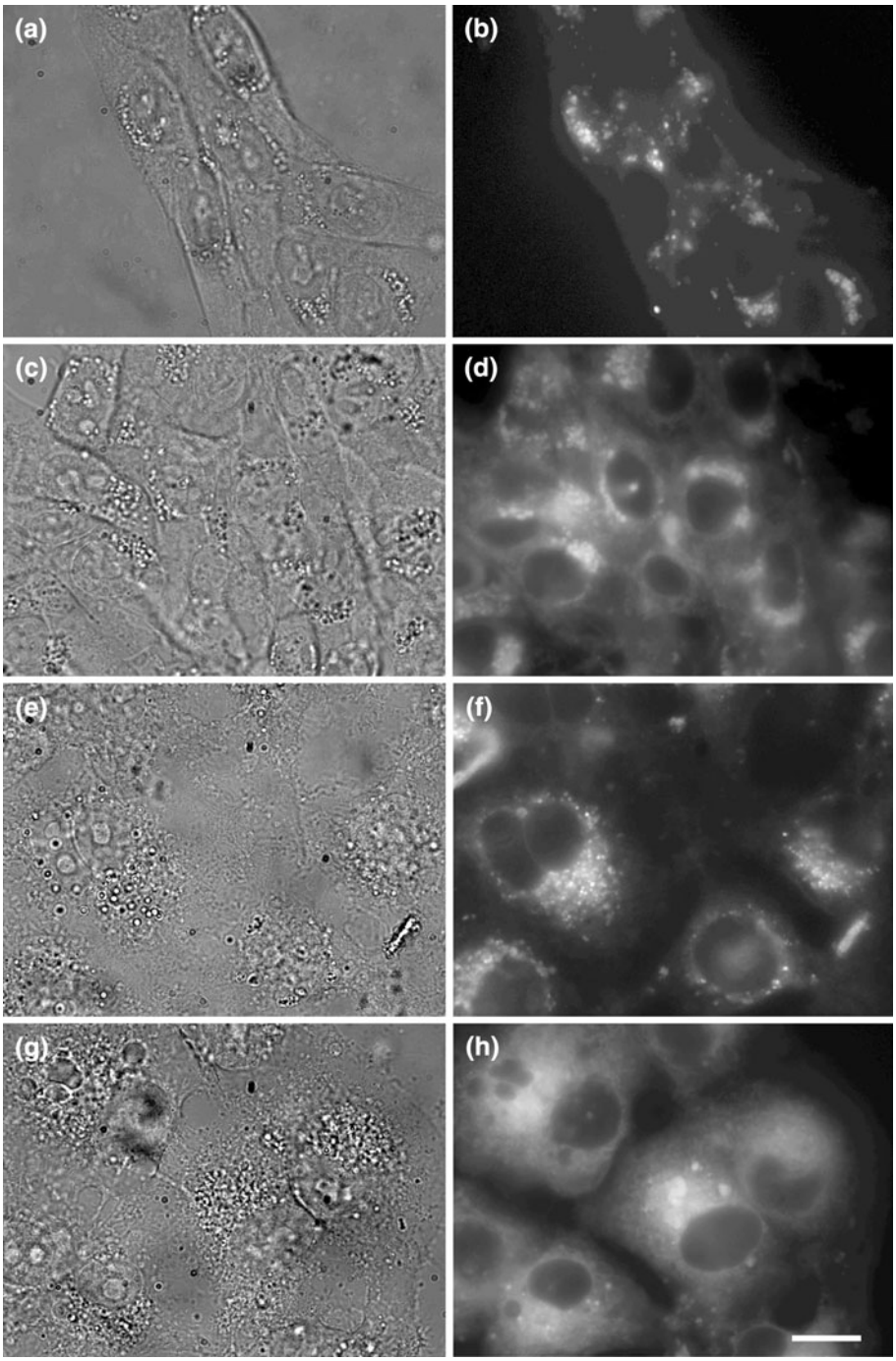

Fig. 7 Microphotographs of 4451 (**a**–**d**) and Nt8e cells (**e**–**h**) incubated with 5.0 μM Cp_6 or Cp_6-his in growth medium. *Left panel* bright fieled images of the cells, *right panel* corresponding fluorescence images showing localization of Cp_6 (**b**, **f**) and Cp_6-his (**d**, **h**). Magnification ×100, *Bar* 20 μM

the conjugate was measured in presence of pheniramine and ranitidine, which are known antagonist for H1 and H2 histamine receptors, respectively. In both the cell lines, these antagonists at 100 μM led to significant inhibition in the cellular uptake of Cp_6-his and the inhibition was more pronounced in the presence of ranitidine, a potent H2 receptor antagonists, suggesting that at least a part of cellular uptake or binding of the conjugate occurred via H2 receptors. Using western blot, we found that H2R receptor is expressed in both the cell lines. However, since higher concentration of the antagonist did not lead to further inhibition in the uptake of the Cp_6-his, the possibility that receptor-independent mechanism also contribute to its intracellular uptake can not be ruled out. Indeed, some histamine agonist, antagonist and BODIPY FL histamine, a fluorophore used to label histamine receptors, have also been shown to be internalized and sequestered in cells by a receptor-independent mechanism [25]. Therefore, to further confirm that the uptake is receptor mediated, the effect of low temperature on cellular uptake of both Cp_6-his and Cp_6 was studied.

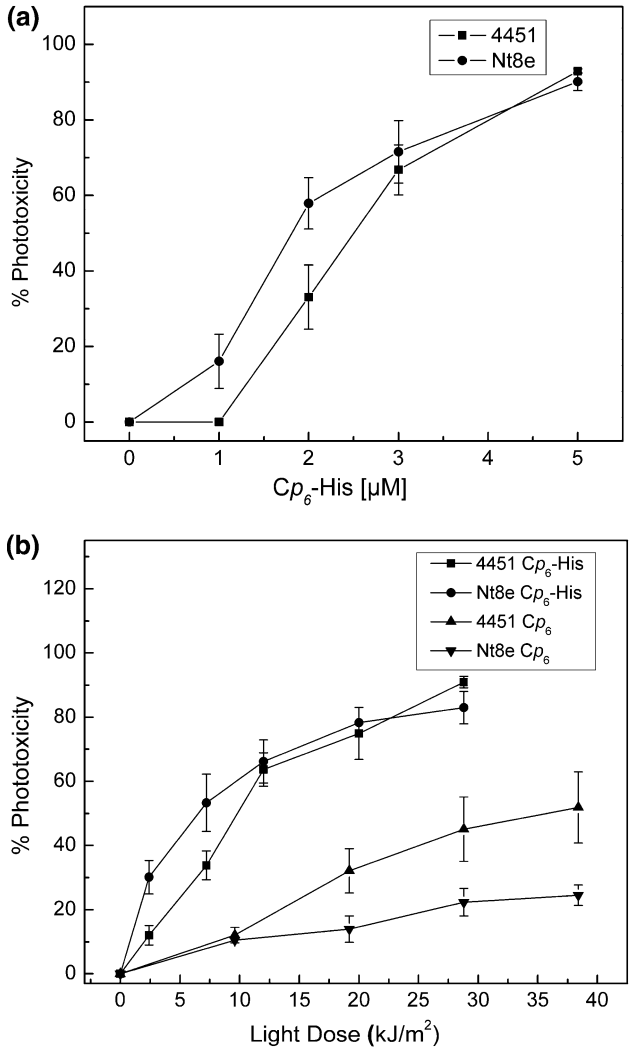

Fig. 8 Percent phototoxicity induced by Cp_6-his at varying concentration from 1-5 μM and fixed light dose at 28 kJ/m^2 (**a**) and both Cp_6 and Cp_6-his conjugate at fixed concentration 5 μM with varying light dose from 0 to 38 kJ/m^2 in 4451 and Nt8e cells (**b**). Cells were incubated for 3 h with photosensitizer in growth medium and irradiated with respective light dose. Phototoxicity was calculated as percent decrease in MTT reduction with respect to a control sample, which received no photosensitizer and no light. The zero dose point shows phototoxicity in cell sample incubated with photosensitizer but not exposed to light. Each data point represents the average ± SD values obtained from three independent experiments

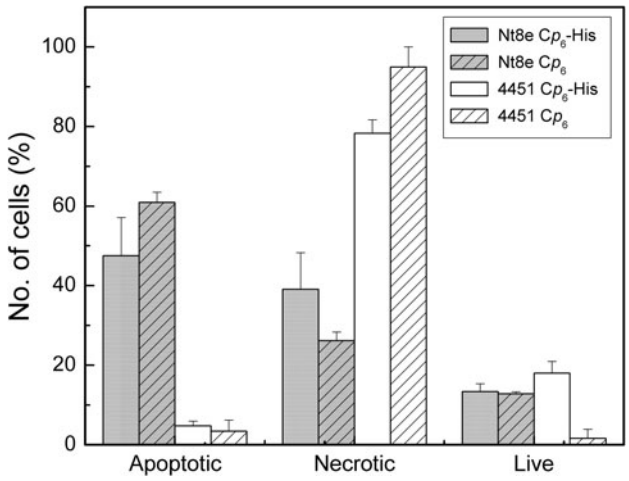

Fig. 9 Percentage of apoptotic and necrotic cells in 4451 and Nt8e cells after 18 h of photodynamic treatment with C$p_6$or Cp_6-his. Cp_6 was used at 10.0 μM with light dose 38 kJ/m^2 and for Cp_6-his, 5.0 μM concentration and ~28 kJ/m^2 was used to obtain ~95% phototoxicity in both the cases. Each data point represents the average ± SD values obtained from three independent experiments

Interestingly, incubation at 15°C led to inhibition of cellular uptake of both the photosensitizers (Fig. 5a). Although the magnitude of inhibition for Cp_6 was slightly lower than Cp_6-his, it was not unexpected due to the fact that hydrophilic Cp_6 via interaction with serum LDLs can also be taken up by receptor-mediated endocytosis [21]. To check this possibility, we omitted serum from the culture media during the incubation period. Results show that the inhibition of cellular uptake due to lower temperature is persistent for Cp_6-his, but in case of Cp_6, it is almost diminished (Fig. 5b).

These results confirmed that the uptake of Cp_6-his is indeed receptor mediated. Apart from histamine receptors, there also exists membrane-associated organic cation transporters (OCTs) that function to remove excess amount of histamine from the extra-cellular space by its re-uptake and transport into the cytoplasm to a yet unidentified site where it is metabolized into inactive metabolite N$^{\tau}$-methylhistamine [18]. However, studies in murine hematopoietic progenitor cells and basophiles have shown that the uptake of histamine by OCT is not affected by the presence of H1 or H2 receptor antagonist [19, 20]. Since we found significant inhibition in uptake of Cp_6-his by histamine antagonist, the possibility of role of OCTs in its cellular uptake is less likely. Since attachment of Cp_6 to histamine can lead to alterations in its physicochemical properties such as relative hydrophobicity, molecular charge and amphiphilicity, one would expect this also to contribute to the improved cellular uptake of Cp_6-his in a manner similar to reported for N-aspartyl ce6 (MACE, LS11) a conjugate of chlorin e6 with aspartic acid [26].

Our results on intracellular localization show that in both the cell lines, Cp_6-his localizes on the cell membrane and also inside the cells in the form of vesicles near the perinuclear region. This is similar to the intracellular localization of histamine reported earlier in rat immune cells [27]. In contrast, the intracellular localization of Cp_6 was distinctly different and occurred in the form of punctuated granular structures inside cytoplasm indicating its localization at multiple sites, such as endoplasmic reticulum, golgi apparatus and lysosomes. This is consistent with our previous studies [28]. The uptake of Cp_6-his via histamine H2 receptor would lead to its accumulation in endosome/lysosome

pool. This due to the fact that histamine H2 receptor is G protein-coupled receptor (GPCRs) which when binds to agonist or antagonist undergoes internalization through the process of endocytosis, resulting in its accumulation in the perinuclear endosomal pool and subsequent trafficking to the lysosomes [22]. The receptor is either recycled back to the plasma membrane or undergoes proteolytic degradation for down regulation [23]. For GPCRs, which utilize endocytosis machinery for receptor regulation, it is generally believed that the receptor and ligand are internalized together [29]. It is therefore likely that the vesicles in the perinuclear region where Cp_6-his is localized represents the endosome/lysosome compartments. Intracellular binding site of histamine to microsomal cytochrome P450 and nucleus have also been identified through which histamine is believed to regulate cell growth and homeostasis [24]. These binding sites designated as H_{IC} are not specific because it can interact with several other compounds also, such as imidazoles (including HA, l-histidine, histidinol), polyamines (putrescine, spermidine, spermine) and hormones (androgens, estrogens, progestins and, to a lesser extent, adrenal steroids) [24]. However, we did not find localization of Cp_6-his in the cell nucleus. The identification of the exact site of Cp_6-his localization needs further investigations.

Phototoxicity and mode of cell death

The results presented in Fig. 8 show that the phototoxicity induced by Cp_6-his was ~4 times higher when compared to Cp_6, whereas the magnitude of increase in the uptake of the conjugate was ~10 times higher than free Cp_6. One important factor that can contribute to this observation is that the absorption coefficient of the conjugate was ~1/2 than Cp_6 at 660 nm. Since the mode of PDT-induced cell death is determined by the intracellular localization of the photosensitizer [30] and significant differences were observed in the intercellular localization of Cp_6 and Cp_6-his, we also investigated the cell death response induced by the two photosensitizers. Measurements on the percentage of apoptotic and necrotic cells after PDT with Cp_6 and Cp_6-his (Fig. 9) showed no difference except that in case of Cp_6-his a slight increase in necrotic cells was observed, which can be attributed to the observed localization of Cp_6-his on the cell membrane. The reasons for the differences in the PDT-induced cell death response observed between the two cell lines may be because of their p53 status. While the 4451 cells is reported to be a p53 mutant [31], the cell line Nt8e contains wild type p53 [32]. The tumor suppressor gene p53 is known for its ability to induce apoptosis by activating downstream cell death effectors including bax, Puma and Noxa [33, 34]. In an study on PDT with hematoporphyrin derivative (HpD), similar results have been reported in 4451 cells and in cell line BMG-1 having wild type p53 [31].

To conclude, the results of our study show that conjugating Cp_6 to histamine improves its cellular uptake and hence the PDT efficacy in oral cancer cell lines. The observations that the cellular uptake of Cp_6-his is significantly inhibited by ranitidine and lower temperature suggest that part of its uptake occurred via histamine receptors. Further, in both the cell lines, the cell death response induced by Cp_6-his was similar to Cp_6. In 4451 cells, cell death was observed to be necrotic type; for Nt8e cells, both apoptosis and necrosis contribute equally to the phototoxicity. We suggest histamine can be used as a carrier for targeted delivery of photosensitizer in cancer cells and to improve PDT efficacy.

Acknowledgments Authors would like to thank Dr. A. Datta, IIT Mumbai for mass spectroscopy measurements, Dr. BS Dwarakanath, INMAS, Delhi and Dr. R Mulherkar, ACTREC, Mumbai for providing oral cancer cell line.

References

1. Brown SB, Brown EA, Walker I (2004) The present and future role of photodynamic therapy in cancer treatment. Lancet Oncol 5:497–508
2. Wilson BC, Patterson MS (2008) The physics, biophysics and technology of photodynamic therapy. Phys Med Biol 53:R61–R109
3. Nyman ES, Hynninen PH (2004) Research advances in the use of tetrapyrrolic photosensitizers for photodynamic therapy. J Photochem Photobiol B Biol 73:1–28
4. Dube A, Sharma S, Gupta PK (2006) Evaluation of chlorin p6 for photodynamic treatment of squamous cell carcinoma in the hamster cheek pouch model. Oral Oncol 42:77–82
5. Sharman WM, van Lier JE, Allen CM (2004) Targeted photodynamic therapy via receptor mediated delivery systems. Adv Drug Delv Rev 56:53–76
6. Chen B, Pogue BW, Hoopes PJ, Hasan T (2006) Vascular and cellular targeting for photodynamic therapy. Crit Rev Eukaryot Gene Expr 16:279–305
7. Schneider E, Rolli-Derkinderen M, Arock M, Dy M (2002) Trends in histamine research: new functions during immune responses and hematopoiesis. Trends Immunol 23:255–263
8. Bartholeyns J, Fozard JR (1985) Role of histamine in tumor development. Trends Pharmacol Sci 6:123–125
9. Medina MA, Quesada AR, de Núñez Castro I, Sánchez-Jiménez F (1999) Histamine, polyamines, and cancer. Biochem Pharmacol 57:1341–1344
10. Rivera ES, Cricco GP, Engel NI, Fitzsimons CP, Martín GA, Bergoc RM (2000) Histamine as an autocrine growth factor: an unusual role for a widespread mediator. Semin Cancer Biol 10:15–23
11. Pós Z, Sáfrány G, Müller K, Tóth S, Falus A, Hegyesi H (2005) Phenotypic profiling of engineered mouse melanomas with manipulated histamine production identifies histamine H2 receptor and rho-C as histamine-regulated melanoma progression markers. Cancer Res 65:4458–4466
12. Medina VA, Rivera ES (2010) Histamine receptors and cancer pharmacology. Br J Pharmacol 161:755–767
13. Szabó PM, Wiener Z, Tömböl Z, Kovács A, Pócza P, Horányi J, Kulka J, Riesz P, Tóth M, Patócs A, Gaillard RC, Falus A, Rácz K, Igaz P (2009) Differences in the expression of histamine-related

genes and proteins in normal human adrenal cortex and adrenocortical tumors. Virchows Arch 455:133–142
14. Hoober JK, Sery TW, Yamamoto N (1988) Photodynamic sensitizers from chlorophyll: purpurin-18 and chlorin p6. Photochem Photobiol 48:579–582
15. Mosman T (1983) Rapid colorimetric assay for cellular growth and survival application and cytotoxicity assays. J Immunol Methods 65:55–63
16. Fukushima Y, Asano T, Saitoh T, Anai M, Funaki M, Ogihara T, Katagiri H, Matsuhashi N, Yazaki Y, Sugano K (1997) Oligomer formation of histamine H2 receptors expressed in Sf9 and COS7 cells. FEBS Lett 409:283–286
17. Van der Goot H, Timmerman H (2000) Selective ligands as tools to study histamine receptors. Eur J Med Chem 35:5–20
18. Ogasawara M, Yamauchi K, Satoh Y, Yamaji R, Inui K, Jonker J, Schinkel A, Maeyama K (2006) Recent advances in molecular pharmacology of the histamine systems: organic cation transporters as a histamine transporter and histamine metabolism. J Pharmacol Sci 101:24–30
19. Corbel S, Traiffort E, Stark H, Schunack W, Dy M (1997) Binding of histamine H3-receptor antagonists to hematopoietic progenitor cells—evidence for a histamine transporter unrelated to histamine H3 receptors. FEBS Lett 404:289–293
20. Schneider E, Machavoine F, Pléau J, Bertron A, Thurmond R, Ohtsu H, Watanabe T, Schinkel A, Dy M (2005) Organic cation transporter 3 modulates murine basophil functions by controlling intracellular histamine levels. JEM 202:387–393
21. Mojzisova H, Bonneau S, Vever-Bizet C, Brault D (2007) Cellular uptake and subcellular distribution of chlorin e6 as functions of pH and interactions with membranes and lipoproteins. Biochim Biophys Acta 1768:2748–2756
22. Fernandez N, Monczor F, Baldi A, Davio C, Shayo C (2008) Histamine H2 receptor trafficking: role of arrestin, dynamin, and clathrin in histamine H2 receptor internalization. Mol Pharmacol 74:1109–1118
23. Osawa S, Kajimura M, Yamamoto S, Ikuma M, Mochizuki C, Iwasaki H, Hishida A, Terakawa S (2005) Alteration of intracellular histamine H2 receptor cycling precedes antagonist-induced upregulation. Am J Physiol Gastrointest Liver Physiol 289:G880–G889
24. LaBella FS, Brandes LJ (2000) Interaction of histamine and other bioamines with cytochromes P450: implications for cell growth modulation and chemopotentiation by drugs. Semin Cancer Biol 10:47–53
25. Morissette G, Lodge R, Bouthillier J, Marceau F (2008) Receptor-independent, vacuolar ATPase-mediated cellular uptake of histamine receptor-1 ligands: possible origin of pharmacological distortions and side effects. Toxicol Appl Pharmacol 229:320–331
26. Kessel D (1989) Determinants of photosensitization by mono–L-aspartyl chlorin e6. Photochem Photobiol 49:447–452
27. Csaba G, Kovács P (2006) Perinuclear localization of biogenic amines (serotonin and histamine) in rat immune cells. Cell Biol Int 30:861–865
28. Begum G, Dube A, Joshi PG, Gupta PK, Joshi NB (2009) Chlorin p6 preferentially localizes in endoplasmic reticulum and golgi apparatus and inhibits Ca^{2+} release from intracellular store. J Photochem Photobiol B Biol 95:177–184
29. Koenig JA (2004) Signal reception: G protein-coupled receptors. In: Davies RW, Morris BJ (eds) Molecular biology of neurons, 2nd edn. Oxford, New York, pp 215–248
30. Plaetzer K, Kiesslich T, Verwanger T, Krammer B (2003) The modes of cell death induced by PDT: an Overview. Med Laser Appl 18:7–19
31. Gupta S, Dwarakanath BS, Muralidhar K, Jain V (2003) Cellular uptake, localization and photodynamic effects of haematoporphyrin derivative in human glioma and squamous carcinoma cell lines. J Photochem Photobiol B Biol 69:107–120
32. Mulherkar R, Goud AP, Wagle AS, Naresh KN, Mahimkar MB, Thomas SM, Pradhan SA, Deo MG (1997) Establishment of a human squamous cell carcinoma cell line of the upper aero-digestive tract. Cancer Lett 118:115–121
33. Burns TF, El-Deiry WS (1999) The p53 pathway and apoptosis. J Cell Physiol 181:231–239
34. Sax JK, El-Deiry WS (2003) p53 downstream targets and chemosensitivity. Cell Death Differ 10:413–417